J. Fluid Mech. (1979), *vol.* 90, *part* 2, *pp.* 257–271
Printed in Great Britain

Influence of the amplitude of a solid wavy wall on a turbulent flow. Part 2. Separated flows

By DANIEL P. ZILKER AND THOMAS J. HANRATTY

Department of Chemical Engineering, University of Illinois, Urbana

(Received 2 May 1977 and in revised form 20 July 1978)

A study has been carried out of turbulent flow over a sinusoidally shaped solid boundary of large enough amplitude that the flow separates from the downstream side of the wave. Measurements are presented of the conditions under which separated flows exist, the extent of the separated region and the variation of the pressure and shear stress along and the velocity profile above the wavy surface. The results are consistent with the model *D* turbulent solution of the linear momentum equations discussed in Zilker, Cook & Hanratty (1977, hereafter referred to as I) in that reversed flows are possible for wave height to wavelength ratios $2a/\lambda > 0{\cdot}033$ and in that the range of flow rates for which reversed flows exist increases with increasing $2a/\lambda$. For non-separated flows and for flows with thin separated regions the amplitude of the pressure variation changes linearly with wave height; however, for very large amplitude waves with thick separated regions it is much less sensitive to variations in wave height since the external flow that controls the pressure variation sees a wave profile consisting of a composite of the solid wave and the separated region. The variation of the velocity field along the wave surface in the non-separated region is similar to that predicted by linear theory for small amplitude waves. The flow separates in a region of increasing pressure and reattaches in the region where the pressure on the wave surface is a maximum. A large increase in the wall shear stress is noted immediately downstream of reattachment.

1. Introduction

A wavy wall bounding a turbulent flow introduces disturbances which cause spatial variation of the flow field and of the shear stress and pressure along the wave surface. Because of the importance of this interaction in determining wave generation on liquid surfaces, sediment transport and flow resistance, considerable attention has been given to the problem of predicting the wave-induced flow over a sinusoidally shaped boundary.

In I measurements were presented of the shear-stress and pressure variation along a solid wave boundary which show the influence of wave amplitude under conditions in which a separated flow does not exist. Pressure measurements indicate an approximately linear response in that the spatial variation is described quite well by a single harmonic with a wavelength equal to that of the wave surface. However, the variation of the wall shear stress τ_w shows a nonlinear behaviour for $au^*/\nu \geqslant 27$, in that this variation can be much more rapid on the leeward side of the wave.

Investigators	Wavelength, λ	Height/length, $2a/\lambda$	Reynolds number, $\lambda U/\nu$	Fluid	Measurements
Stanton *et al.* (1932)	2·6 cm 7·6 cm	0·4 0·4	23 400, 70 600 24 000	Air	Wall pressure
Motzfield (1937)	30 cm 30 cm	0·05 0·1	330 000 330 000	Air	Pressure Average velocity
Zagustin *et al.* (1966)	3 ft 2 ft	0·042 0·021	147 000, 317 000 147 000, 317 000	Water	Wall pressure, wall shear stress, average velocity over crest
Sigal (1971)	6 in. 12 in.	0·052 0·056	154 000, 306 000 154 000, 306 000	Air	Pressure, wall shear stress, average velocity, fluctuating velocities
Kendall (1970)	4 in.	0·062	19 000 to 64 000	Air	Pressure, wall shear stress, fluctuating velocities, average velocity at two locations
Beebe (1972)	4·2 in.	0·17 0·40	21 400 to 85 600 21 400 to 85 600	Air	Pressure, wall shear, visual studies, average velocity over crest, fluctuating velocities
Hsu & Kennedy (1971)	0·833 ft 1·667 ft	0·044 0·022	238 000 to 476 000 238 000 to 476 000	Air	Pressure, wall shear, average velocity, fluctuating velocities
Thorsness *et al.* (1978)	2 in.	0·012	11 000 to 64 000	Water	Wall shear
Zilker *et al.* (1977, i.e. I) Zilker (1976) Cook (1970)	2 in.	0·012, 0·0312, 0·05	11 000 to 64 000	Water	Wall pressure, wall shear stress, average velocity, fluctuating velocities, visual studies
Present study Zilker (1976) Cook (1970)	2 in.	0·05, 0·125, 0·200	11 000 to 64 000	Water	Wall pressure, wall shear stress, average velocity, fluctuating velocities, visual studies

TABLE 1. Summary of experimental studies of flow over a train of stationary sinusoidal waves.

These results suggest that for non-separated flows most of the flow field can be described by solutions of linearized momentum equations. Nonlinear effects need to be taken into account only very close to the solid boundary. A turbulent solution of the linear momentum equations developed by Thorsness (1975), Thorsness & Hanratty (1977) and Thorsness, Morrisroe & Hanratty (1978) describes quite well the phase and amplitude of the pressure and the first harmonic of the shear-stress profile and the velocity field outside the viscous wall region. A summary of this analysis is present in I.

This paper is an extension of work described in I in that we examine the influence of the amplitude of a solid wavy wall when a separated flow exists. Measurements are presented of the conditions under which separated flow exists, the extent of the separated region and the variation of the pressure and shear stress along and the velocity profile above the wavy surface. A summary of previous studies of flow over trains of sinusoidally shaped stationary waves is given in table 1. The work presented in this paper plus that presented in I represents the most comprehensive study of the influence of the wave height and flow rate. In addition, the rather careful effort to establish when separation occurs and the extent of the separated region has enabled us to relate in a more definite way the observed variations of the wall pressure, wall shear stress and average velocity to properties of the separated flow.

Most of the theoretical work on flow over wavy surfaces has involved solutions of the linear momentum equations. Recently finite-difference solutions of the non-linear momentum equations have been presented by Taylor, Gent & Keen (1976) for situations in which the average velocity is in the forward direction throughout the flow field. At present a method for analysing flows with a separated region does not exist.

The study described in this paper was carried out to obtain results which would guide such an analysis. The measurements were largely motivated by the motion that one must consider three aspects of the flow: the separated region, the external region and the boundary layer along that part of the wave surface exposed to a forward-moving flow. The results presented in I suggest to us that the external flow and pressure variation can be calculated by solving the linear momentum equations for flow over a composite boundary consisting of the stationary wave boundary and the forward-moving outer boundary of the separated region. They also suggest that a boundary-layer assumption can be made for the portion of the wave surface exposed to a forward-moving flow since viscous and turbulent stresses are important only in a thin region close to surface where the pressure is varying only in the flow direction. The results presented in this paper support such an approach.

2. Description of experiments

The apparatus in which the experiments were conducted and the techniques used to carry out the measurements are described in I.

An electrolyte was circulated through a flow loop that contained a 8·38 m channel with a 5·08 by 60·96 cm rectangular cross-section. The test section was located at the downstream end of the channel, where a fully developed turbulent flow existed. The bottom portion consisted of a removable 60·96 by 68·58 cm test plate which contained the waves to be studied. Three different waves with height-to-length ratios $2a/\lambda$ of

0·05, 0·125 and 0·200 were constructed from Plexiglas and had ten crests separated by a distance of 5·08 cm. The results presented in this paper were obtained over the fifth wave for $2a/\lambda = 0{\cdot}05$, the fifth, sixth, ninth and tenth waves for $2a/\lambda = 0{\cdot}125$ and the eighth and ninth waves for $2a/\lambda = 0{\cdot}200$.

The pressure variation along the wave surface was determined using taps connected to 0·084 cm holes in the wave surface. Visual studies of the flow pattern were carried out by injecting dye through these pressure taps.

The wall shear stress was determined by measuring the mass-transfer rate to flush-mounted electrodes located along the wave surface. This electrochemical technical can give the magnitude of the wall shear stress only in regions where the flow is not changing direction with time. The regions of forward flow were determined by observing the motion of dye injected at the surface and by using sandwich electrodes developed by Son & Hanratty (1969). These consisted of two rectangular electrodes sandwiched together with a thin layer of insulation and mounted in the wave surface with their long side perpendicular to the direction of mean flow. The difference in the signal from the electrodes indicates the flow direction, since the smaller mass-transfer rate is registered by the downstream electrode. Measurements of the time-averaged wall shear stress could not be made in the separated region since the wall stress fluctuations were too large compared with the time-averaged wall stress.

The average velocity in the fluid was determined by a 1287-EW split-film thermal probe manufactured by Thermo-Systems. From the readings of the two films we determined the velocity component U in the direction of mean flow and the tangent of the angle that the streamline makes with the direction of mean flow. The probe was attached to a traversing mechanism which moved vertically downwards from the top wall. Provisions were made so that traverses could be made at ten different locations between the eighth and tenth waves.

3. Results

3.1. *Parameterization*

The manner in which the flow varies along the surface depends on the wave amplitude and the flow rate. We characterize the flow rate by a Reynolds number hU_b/ν or by a dimensionless wavenumber $\alpha\nu/u^*$ when comparisons are made with linear theory. Here h is the half-height of the channel and U_b is the bulk average velocity defined by the velocity profile measured at the centre of the channel when the wave section is replaced by a flat section:

$$U_b = \frac{1}{h}\int_0^h \bar{U}\,dy. \tag{1}$$

The friction velocity $u^* = (\tau_s/\rho)^{\frac{1}{2}}$ is defined in terms of the wall shear stress that would exist if the wave section were replaced by a flat section.

3.2. *Visual studies*

Figures 1 (*a*)–(*d*) (plates 1–4) show examples of photographs of dye-streamer studies with a wave of height-to-length ratio $2a/\lambda = 0{\cdot}125$. These photographs show a separated region from $x/\lambda = 0{\cdot}1$ to $x/\lambda = 0{\cdot}6$.

Figure 1 (*a*) (plate 1) shows the trace of a dye streamer originating from an injection point at a streamwise location of $0{\cdot}7\,x/\lambda$. This streamer travels in a forward direction close to the wave surface from the point of injection until just beyond the wave crest, where it diverges from the surface. Injection of the dye at the wave crest permitted a closer examination of the separation point as indicated in figure 1(*b*) (plate 2). This photograph reveals that the flow continues along the wave surface until it reaches the separation point, where it is forced rapidly upwards, away from the wave surface, by the recirculating reverse flow near the wall close to the separation point. Figure 1(*c*) (plate 3) shows a dye streamer injected downstream of the separation point. Fluid close to the wave surface is moving against the direction of mean flow. This figure also shows alternating bands of dye oriented normal to the wave surface similar to dye patterns found in the wake of a cylinder in cross-flow. Figure 1(*d*) (plate 4) shows the dye pattern obtained by injecting dye at the trough. It displays the swirling nature of the flow in this region of the wave surface. The dye is split into two streamers: one which moves along the surface in the direction of mean flow and a larger dye streamer which moves against the direction of bulk flow. The dye patterns in this region are quite variable but in general they seem to alternate between a completely forward flow and the one shown in figure 1(*d*).

Visual studies with the larger amplitude wave with $2a/\lambda = 0{\cdot}20$ showed the same type of behaviour except that the separated region appeared to be much thicker. However, the wave with a height-to-length ratio of $2a/\lambda = 0{\cdot}05$ showed decidedly different behaviour. For this wave reversed flow could be observed only very near the surface. Consequently we have concluded that the thickness of the reversed region is very small.

3.3. *Extent of the separated region*

From the visual studies just described we could determine the approximate location on the wave surface at which the flow changed direction. Actually the change in direction at the surface from a forward-moving to a backward moving flow did not occur at a fixed location but seemed to shift over a maximum distance of $\Delta x = + 0{\cdot}05\lambda$. At some dye taps the dye shifted direction continuously and the flow was called forward moving if on an average the dye moved in the direction of mean flow. The change from a reversed to a forward flow at the surface was more difficult to observe than the change from a forward to a reversed flow since the region over which this change occurred was larger by a factor of about 1·5.

Determinations of the average direction of flow using the sandwich electrodes described in § 2 agreed with results obtained by observing dye streamers. However this technique was not as effective in determining the location where the flow changed direction because it was inconvenient to locate a large number of sandwich electrodes along the wave surface.

We have defined locations for the initiation and termination of reversed flows as the midpoint between two dye ports where, on average, the dye streamer showed definitely different directions. Some typical measurements obtained in this way are summarized in table 2. For comparison we also give in table 2 calculated results from linear theory. The Reynolds stresses used in this calculation were evaluated from the model D discussed in I. The parameter values $k_1 = -60$ and $k_{LP} = 3000$ chosen for the calculations were shown in I to give good agreement with measured wall shear-stress profiles and pressure profiles for small amplitude waves. Approximate agreement is noted.

		x/λ for initiation of reversed flow		x/λ for initiation of forward flow	
Re	Wave surface $2a/\lambda$	Predicted by linear theory	Measured	Predicted by linear theory	Measured
5000	0·05	0·238	0·16	0·499	0·393
15000	0·05	0·239	0·16	0·408	0·393
30000	0·05	None	None	None	None
7500	0·125	0·148	0·12	0·556	0·55
16200	0·125	0·129	0·10	0·513	0·60
31600	0·125	0·127	0·10	0·462	0·55
8300	0·200	0·133	0·10	0·577	0·65
15860	0·200	0·112	0·08	0·5470	0·70

TABLE 2. Reversal of flow at the wave surface.

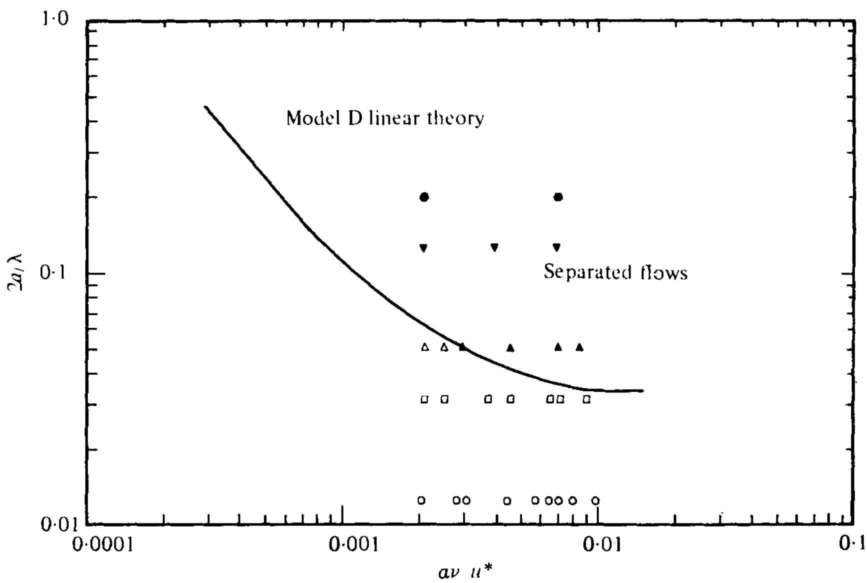

FIGURE 2. Comparison of measured and predicted flow reversals. ◡, $2a/\lambda = 0{\cdot}012$; □, $2a/\lambda = 0{\cdot}031$; △, $2a/\lambda = 0{\cdot}050$; ▽, $2a/\lambda = 0{\cdot}125$; ○ $2a/\lambda = 0{\cdot}200$.

Figure 2 summarizes the conditions under which we have observed reversed flows. The open points represent conditions under which a completely forward-moving flow was observed. The data points for $2a/\lambda = 0{\cdot}012$ and for $2a/\lambda = 0{\cdot}031$ correspond to the conditions for the experimental results reported in I. It is to be noted that for the $2a/\lambda = 0{\cdot}05$ surface the flow changed from a condition where reversed flows did not exist as the Reynolds number increased. For comparison, predictions based on linear theory are presented. The measurements are consistent with the predictions of linear theory that reversed flows are possible for $2a/\lambda > 0{\cdot}033$ and that the range of flow rates for which reversed flows exist increases with increasing $2a/\lambda$. This agreement is surprising since it should not be expected that linear theory is accurate close to a boundary when conditions approach those for a separated flow.

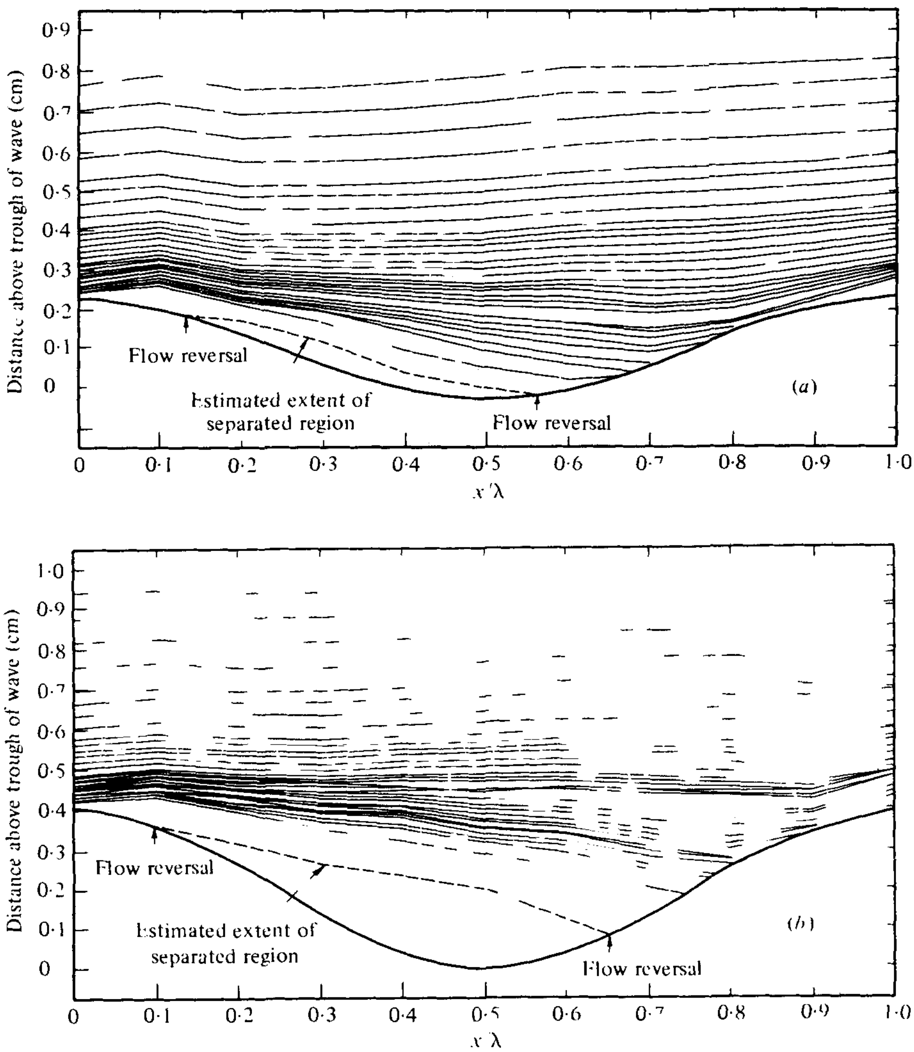

FIGURE 3. Fluid-particle trajectories over a wave surface with (*a*) $2a/\lambda = 0{\cdot}125$ and (*b*) $2a/\lambda = 0{\cdot}200$ at $Re = 800$.

The thickness of the separated region can be estimated from the measurements of the two components of the velocity made with the split-film sensor. From these the magnitude and the direction of the fluid velocity could be calculated at ten locations along the wave for different distances above the surface. An approximate average trajectory for the fluid particle was calculated for particles originating at different positions above the wave crest. This was done by assuming that the particles moved in a straight line to the next position at which measurements were available, $0{\cdot}1\lambda$ away. This calculation was discontinued when the particle either touched the wall or was above the next crest. Examples of these calculations are shown in figure 3(*a*) and (*b*) for waves with $2a/\lambda = 0{\cdot}125$ and $0{\cdot}200$. The positions on the wave surface at which the flow reversed its direction are also indicated. We have approximated the outer edge of the separated region by the dashed lines shown in these figures. These

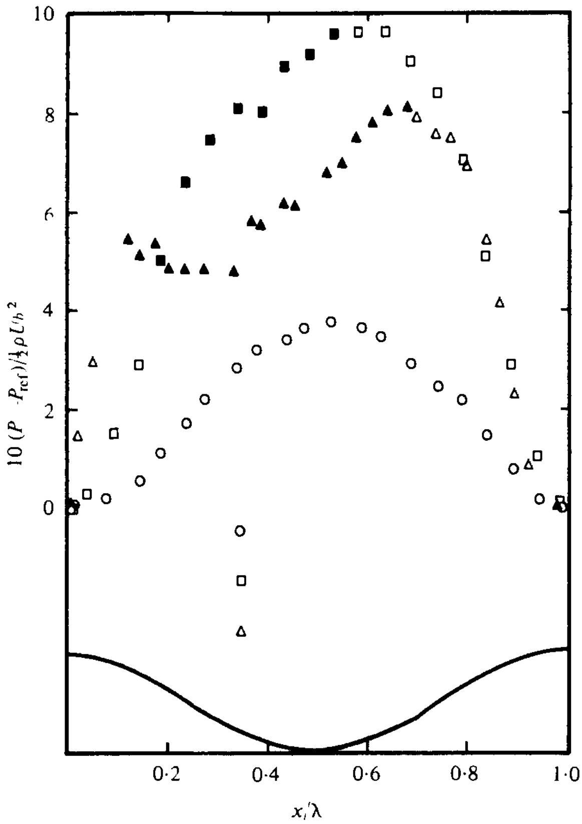

FIGURE 4. Effect of wave amplitude on time-averaged pressure profiles at $Re = 30000$. ○, $2a/\lambda = 0{\cdot}05$; □, $2a/\lambda = 0{\cdot}125$; △, $2a/\lambda = 0{\cdot}200$.

were drawn between the two flow-reversal points in a manner which seemed consistent with the calculated streamlines and the profiles of average velocity discussed in § 3.5.

Motzfield (1937) used the stream function to estimate streamline patterns. We did not use this technique because it would have required an integration of the velocity profile from the wave surface outwards and we were not confident enough of the accuracy of our velocity measurements very close to the wall or in the separated region.

3.4. *Pressure profiles*

Pressure profiles for different wave heights are presented in figure 4 for $Re \simeq 30000$. These clearly show the strong influence of the separated region. The solid symbols indicate locations where the flow direction was found to be reversed at the wave surface.

The wave with $2a/\lambda = 0{\cdot}05$ did not have a reversed flow. The profile is approximated quite well by a cosine function with its maximum displaced slightly downstream from the wave trough. The pressure profile was similar at lower Reynolds number, where a reversed flow was observed on this wave. This is consistent with the visual observations, which indicated that the reversed flow for this wave was confined to a very thin region close to the surface.

$2a/\lambda$	Re	Drag coefficient, C_D
0·05	29300	$1{\cdot}26 \times 10^{-3}$
0·125	14730	$1{\cdot}155 \times 10^{-2}$
	30000	$1{\cdot}003 \times 10^{-2}$
0·200	30530	$1{\cdot}373 \times 10^{-2}$

TABLE 3. Influence of wave height on form drag. $C_D = F_D/\frac{1}{2}\rho U_b^2$.

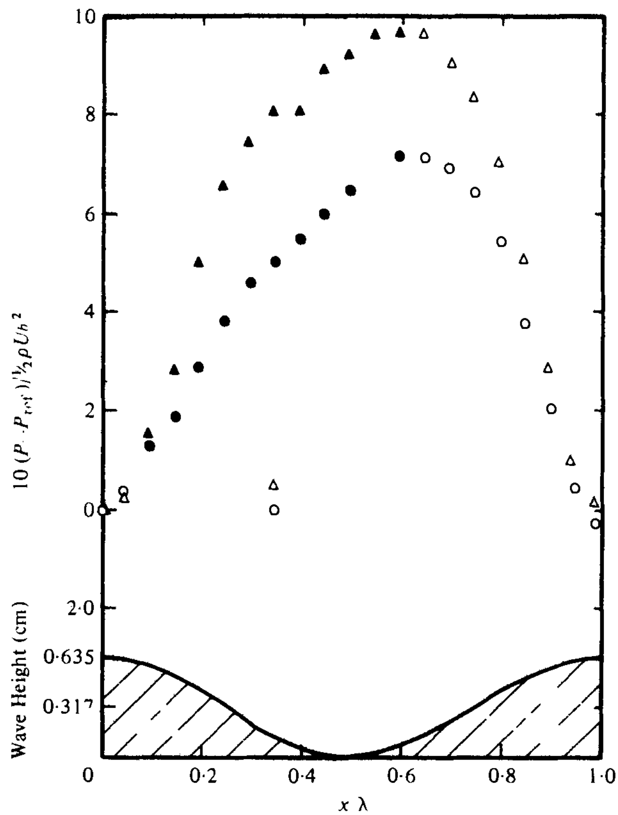

FIGURE 5. Effect of Reynolds number on time-averaged pressure profiles for a wave with $2a/\lambda = 0{\cdot}125$. △, $Re = 30000$; ○, $Re = 14730$.

The pressure profile for the wave with $2a/\lambda = 0{\cdot}125$ was distorted from a cosine function in such a way that the region of decreasing pressure was smaller than the region of increasing pressure. The flow separated in the region of increasing pressure and reattached to the wave surface approximately at the maximum in the pressure profile. Of particular interest is the observation that the increase in wave amplitude from $2a/\lambda = 0{\cdot}05$ to $2a/\lambda = 0{\cdot}125$ caused a proportionate increase in the amplitude of the pressure variation. Apparently the separated region altered the shape but did not significantly change the amplitude of the composite surface consisting of the wave and the separated region. See, for example, the estimated extent of the separated region shown in figure 3 (*a*).

The pressure profile for the wave with $2a/\lambda = 0{\cdot}200$ also shows a peak approxi-

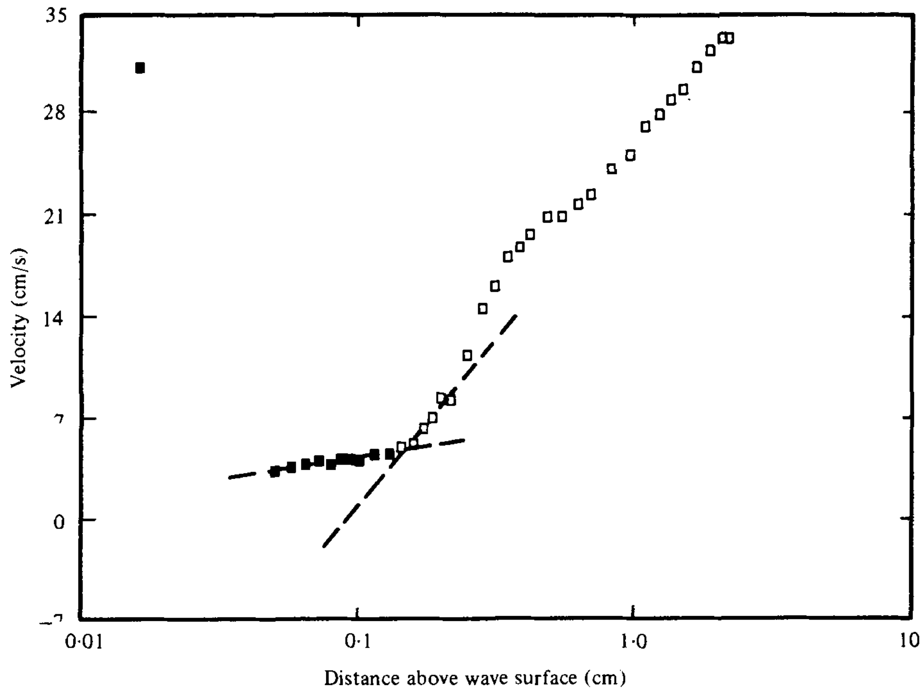

FIGURE 6. Average velocity profiles at $x/\lambda = 0{\cdot}2$ for a wave surface with $2a/\lambda = 0{\cdot}200$. $y_0 = 0{\cdot}12$, $Re = 8000$.

mately at the reattachment point and a region of rising pressure at separation. A plateau in the pressure is noted along the wave surface where we should expect the separated region to be the thickest. (See figure 3*b*.) An increase in wave amplitude from $2a/\lambda = 0{\cdot}125$ to $2a/\lambda = 0{\cdot}200$ causes a decrease in the amplitude of the pressure variation. This can be explained by the existence of a very thick separated region, so that the amplitude of the composite surface 'seen' by the external flow is not much different for $2a/\lambda = 0{\cdot}200$ and $0{\cdot}125$.

Form drags can be calculated from these pressure profiles by evaluating the integral

$$F_D = \int_0^\lambda P \frac{dy}{dx} dx, \tag{2}$$

where $y = a\,e^{i\alpha x}$. These are given in table 3. It is noted that F_D increases with increasing wave height, but that the increase from $2a/\lambda = 0{\cdot}05$ to $2a/\lambda = 0{\cdot}125$ is much more striking than that from $2a/\lambda = 0{\cdot}125$ to $2a/\lambda = 0{\cdot}200$.

The influence of fluid velocity is shown by comparing the pressure profiles for $Re = 30\,000$ and $Re = 14\,730$ in figure 5. It is noted that the shape of the two profiles is the same but that the magnitude of the pressure coefficient is slightly larger for the flow at a larger Reynolds number.

3.5. *Velocity profiles*

The velocity profile measured over a wave with a large separated region is shown in figure 6. The filled symbols lie within the separated region indicated in figure 3(*b*). The interpretation of these data points is uncertain.

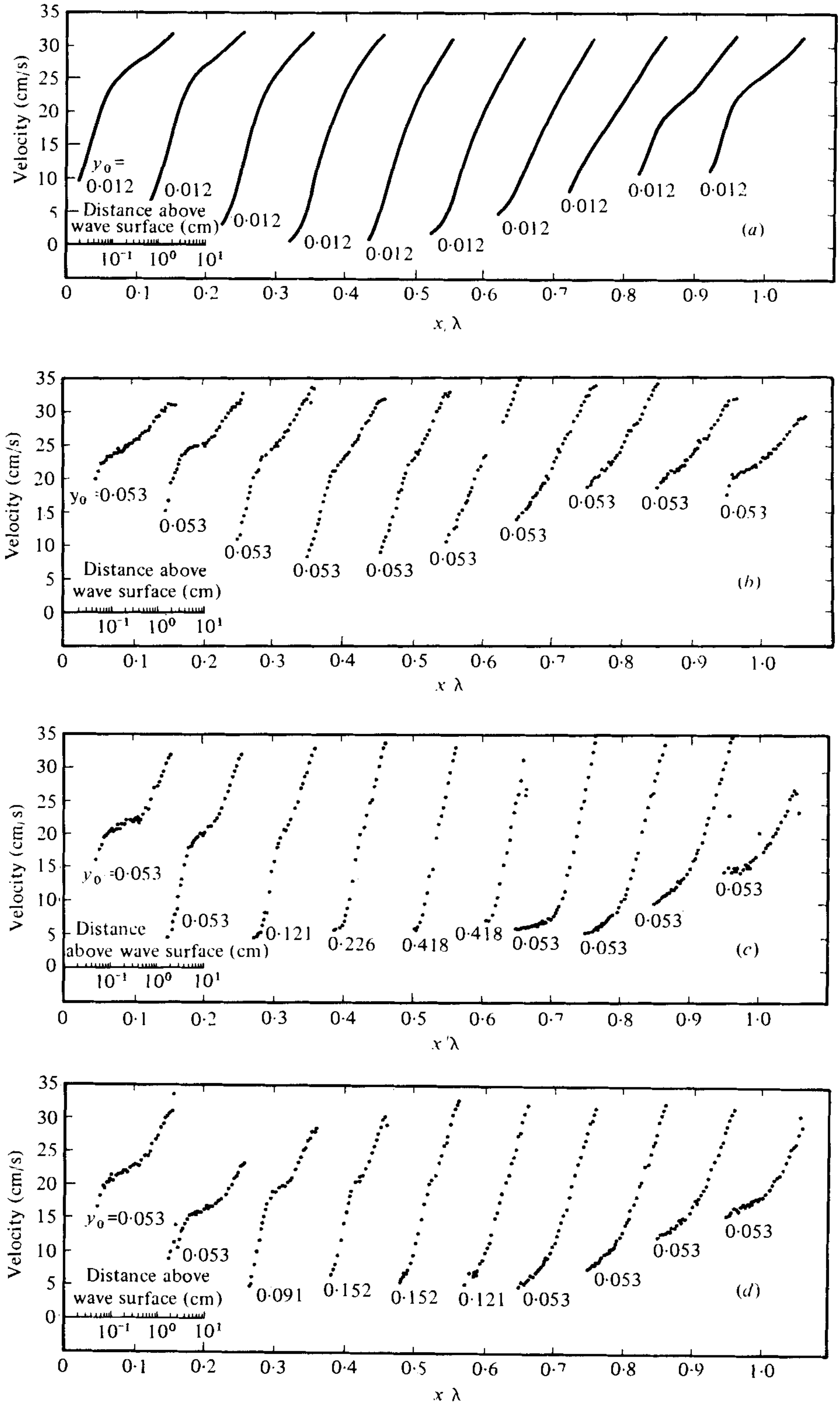

FIGURE 7. (*a*) Model *D* velocity profiles for a wave with $2a/\lambda = 0{\cdot}05$ at $Re = 8000$. (*b*) Velocity profiles in the non-separated region for a wave with $2a/\lambda = 0{\cdot}05$ at $Re = 8000$. (*c*) Velocity profiles in the non-separated region for a wave with $2a/\lambda = 0{\cdot}125$ at $Re = 8000$. (*d*) Velocity profiles in the non-separated region for a wave with $2a/\lambda = 0{\cdot}200$ at $Re = 8000$.

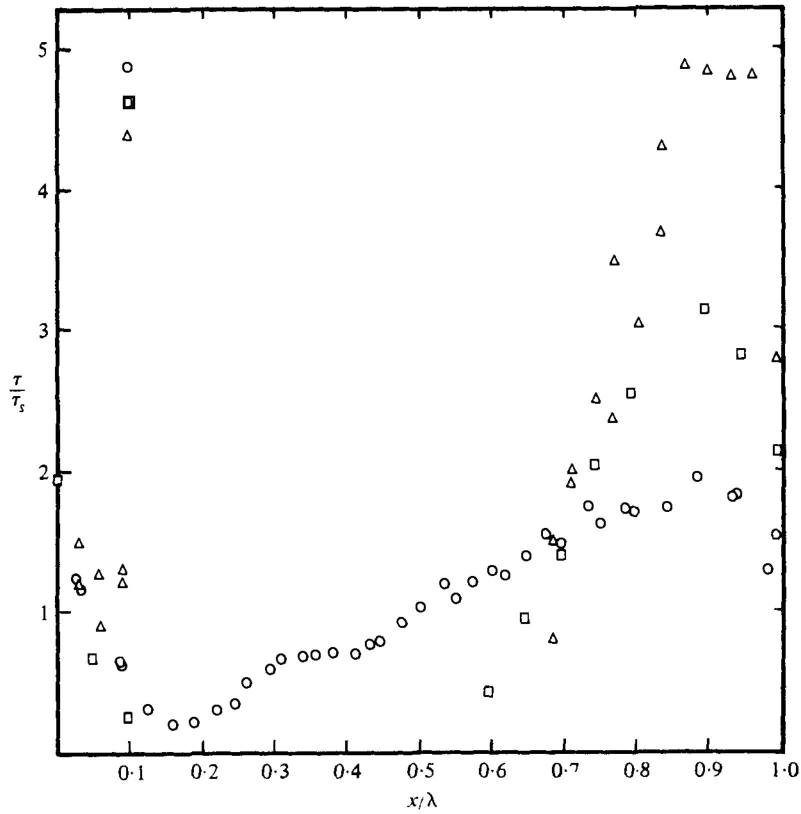

FIGURE 8. Measurements of the wall shear stress for $Re = 31000$. $\bigcirc$, $2a/\lambda = 0{\cdot}05$; $\square$, $2a/\lambda = 0{\cdot}125$; $\triangle$, $2a/\lambda = 0{\cdot}200$.

Our present feeling is that measurements made in the separated region are unreliable since the flow could be so highly agitated that the analysis of the performance of the thermal probes used to measure velocity is no longer correct. It is of interest to note, however, that all of the measured profiles indicated a sharp change in the slope of the velocity profile roughly at the estimated outer boundary of the separated region shown in figures 3 (*a*) and (*b*).

Because of the uncertainty of the interpretation of measurements in the separated region, these have been omitted from the velocity data shown in figures 7 (*b*)–(*d*). Here y_0 is the distance above the wave surface for the lowest point on a profile. For comparison, calculations based on linear theory for a wave with $2a/\lambda = 0{\cdot}05$ are shown in figure 7 (*a*). As already mentioned in § 3.4, turbulence model *D* (described in I) was used to evaluate the turbulent stress. Very dramatic changes in the shape of the velocity profile are noted as the flow progresses along the wave surface. Of particular interest is the similarity in behaviour shown in figures 7 (*a*)–(*d*).

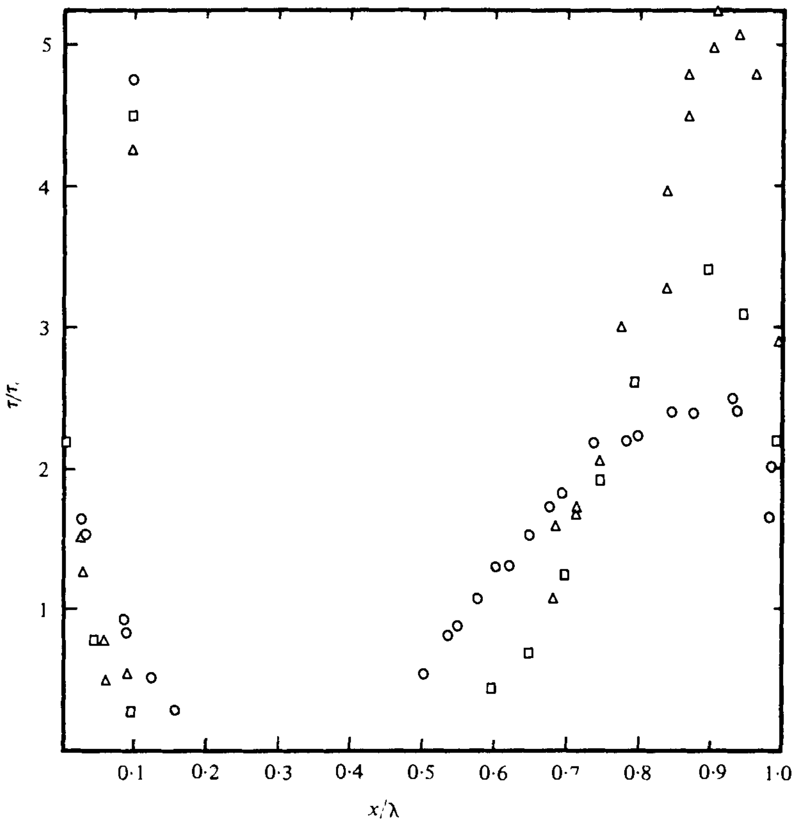

FIGURE 9. Measurements of the wall shear stress for $Re = 6016$–7500. ○, $2a/\lambda = 0{\cdot}05$, $Re = 6016$; □, $2a/\lambda = 0{\cdot}15, Re = 7500$; △, $2a/\lambda = 0{\cdot}200$, $Re = 7180$.

3.6. *Wall shear stress*

Measurements of the wall shear are shown in figures 8 and 9. The striking feature of these measurements is the very rapid increase in the stress shortly after reattachment. They clearly show the type of behaviour to be expected for a boundary-layer flow caused by impingement of a flow on a solid surface.

4. Comparison with previous measurements

A comparison of the results just presented with previously published research gives a rather consistent picture of the influence of the wave height on the characteristics of the flow.

As was pointed out in I, measurements obtained with waves with $2a/\lambda \leqslant 0{\cdot}062$ (Motzfield 1937; Zagustin *et al.* 1966; Sigal 1971; Kendall 1970; Hsu & Kennedy 1971) show symmetric pressure profiles which are close to a sinusoidal shape and which have a maximum at or downstream of the wave trough. The pressure measurements shown in this paper for $2a/\lambda = 0{\cdot}125$, as well as the measurements by Motzfield for $2a/\lambda = 0{\cdot}1$ and by Beebe (1972) for $2a/\lambda = 0{\cdot}17$, show an asymmetric smoothly varying profile, with a more gradual pressure rise on the downstream side of the wave. Our pressure measurements for waves with $2a/\lambda = 0{\cdot}20$, as well as the measurements by Stanton, Marshall & Houghton (1932) for $2a/\lambda = 0{\cdot}4$ and by Beebe for $2a/\lambda = 0{\cdot}40$, show not only asymmetry but also secondary peaks. Our measurements show a single secondary peak while the Stanton *et al.* measurements with $\lambda = 7{\cdot}6$ cm show two secondary peaks. The Beebe measurements and the Stanton *et al.* measurements with $\lambda = 2{\cdot}6$ cm have secondary peaks with such small amplitude that the region of the wall in contact with the separated flow can be considered to be approximately at constant pressure.

As reported in I, the shear-stress profiles show asymmetries for smaller wave heights than do the pressure profiles. Thus in I it was found that for $2a/\lambda = 0{\cdot}0312$ and $0{\cdot}05$ a much more gradual decrease occurred in the wall shear in the trough region than is exhibited by a sine wave. Kendall's measurements with $2a/\lambda = 0{\cdot}062$ and $Re = 33\,000$ show a symmetric pressure profile and an asymmetric shear-stress profile similar to those was reported in I for $2a/\lambda = 0{\cdot}05$ and $Re = 30\,000$. Sigal's measurements with a 12 in. wave indicate symmetric shear-stress and pressure measurements for $h/\lambda = 0{\cdot}056$ at a much higher Reynolds number than was studied in I. This would suggest that the occurrence of asymmetries in the shear-stress profile depends on the Reynolds number. His measurements with a 6 in. wave for $2a/\lambda = 0{\cdot}052$ are puzzling in that they show patterns more similar to those observed here for larger $2a/\lambda$. Measurements of shear-stress profiles for waves of large enough $2a/\lambda$ that asymmetric pressure profiles are obtained (the $2a/\lambda = 0{\cdot}200$ waves discussed in this paper and the $2a/\lambda = 0{\cdot}17$ and $2a/\lambda = 0{\cdot}40$ waves studied by Beebe) show a sharp peak just upstream of the wave crest in regions of the flow which are non-separated.

Our visual studies with $2a/\lambda = 0{\cdot}125$ and $2a/\lambda = 0{\cdot}200$ and those reported by Beebe for $2a/\lambda = 0{\cdot}17$ are in qualitative agreement and show that large variations in the pressure can occur along portions of the wall in contact with a separated region. For larger wave amplitudes (Beebe's results for $2a/\lambda = 0{\cdot}40$) the separated region is quite thick and the pressure variation along the wall is not as great as when it is thinner. Beebe's visual observation that the separation point occurs slightly downstream of the crest in a region of increasing wall pressure is in qualitative agreement with our results. However, our visual techniques enabled us to locate the actual separation point somewhat more accurately than Beebe could.

Our measurements of average velocity for $2a/\lambda = 0{\cdot}05$ reported in this paper and in a previous one by Thorsness *et al.* (1978) are in close agreement with measurements by Sigal for $2a/\lambda = 0{\cdot}052$–$0{\cdot}056$. As shown in the paper by Thorsness *et al.* (1978), qualitatively they agree quite well with predictions by linear theory. Our conclusion from this comparison with linear theory is that, with the exception of a very thin region close to the surface, the wave-induced variations in the average velocity are unaffected by viscous or turbulent stresses. A similar conclusion seems to have been arrived at by Sigal and by Hsu & Kennedy from consideration of total-head measurements.

This work is being supported by the National Science Foundation under Grant NSF ENG 76-22969.

REFERENCES

BEEBE, P. 1972 Turbulent flow over a wavy boundary. Ph.D. thesis, Colorado State University, Fort Collins.

COOK, G. W. 1970 Turbulent flow over solid wavy surfaces. Ph.D. thesis, University of Illinois, Urbana.

HSU, S. T. & KENNEDY, J. F. 1971 *J. Fluid Mech.* **47**, 481.

KENDALL, J. M. 1970 *J. Fluid Mech.* **41**, 259.

MOTZFIELD, H. 1937 *Z. angew. Math. Mech.* **17**, 193.

SIGAL, A. 1971 An experimental investigation of the turbulent boundary layer over a wavy wall. Ph.D. thesis, California Inst. Tech., Pasadena.

SON, J. S. & HANRATTY, T. J. 1969 *J. Fluid Mech.* **35**, 353.

STANTON, T., MARSHALL, D. & HOUGHTON, R. 1932 *Proc. Roy. Soc.* A **137**, 283.

TAYLOR, P. A., GENT, P. R. & KEEN, J. M. 1976 *J. Roy. Astr. Soc.* **44**, 177.

THORSNESS, C. B. 1975 Transport phenomena associated with flows over a solid wavy surface. Ph.D. thesis, Department of Chemical Engineering, University of Illinois, Urbana.

THORSNESS, C. B. & HANRATTY, T. J. 1977 Turbulent flows over wavy surfaces. *Proc. Symp. Turbulent Shear Flows, Penn. State Univ.*

THORSNESS, C. B., MORRISROE, P. E. & HANRATTY, T. J. 1978 *Chem. Engng Sci.* **30**, 579.

ZAGUSTIN, K., HSU, E. Y., STREET, R. L. & PERRY, B. 1966 Flow over a moving boundary in relation to wind-generated waves. *Dept. Civil Engng, Stanford Univ. Tech. Rep.* no. 60.

ZILKER, D. P. 1976 Flow over wave surfaces. Ph.D. thesis, University of Illinois, Urbana.

ZILKER, D. P., COOK, G. W. & HANRATTY, T. J. 1977 *J. Fluid Mech.* **82**, 29.

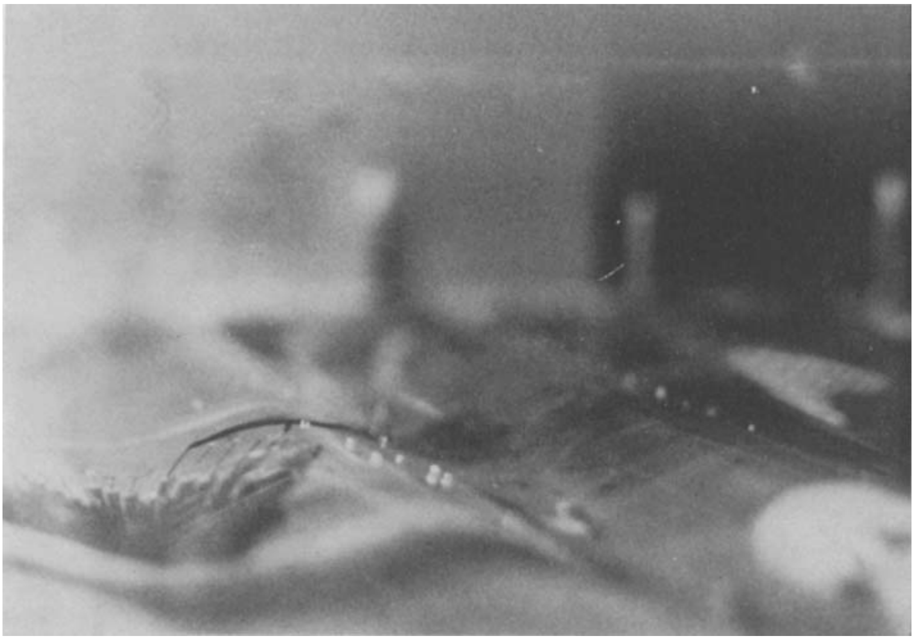

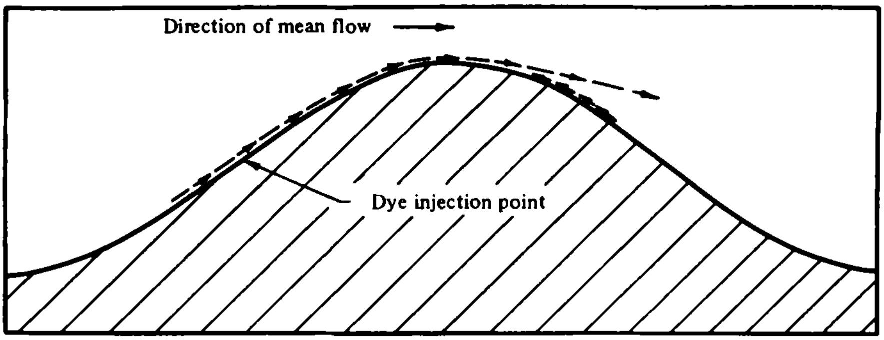

FIGURE 1 (*a*). For legend see plate 4.

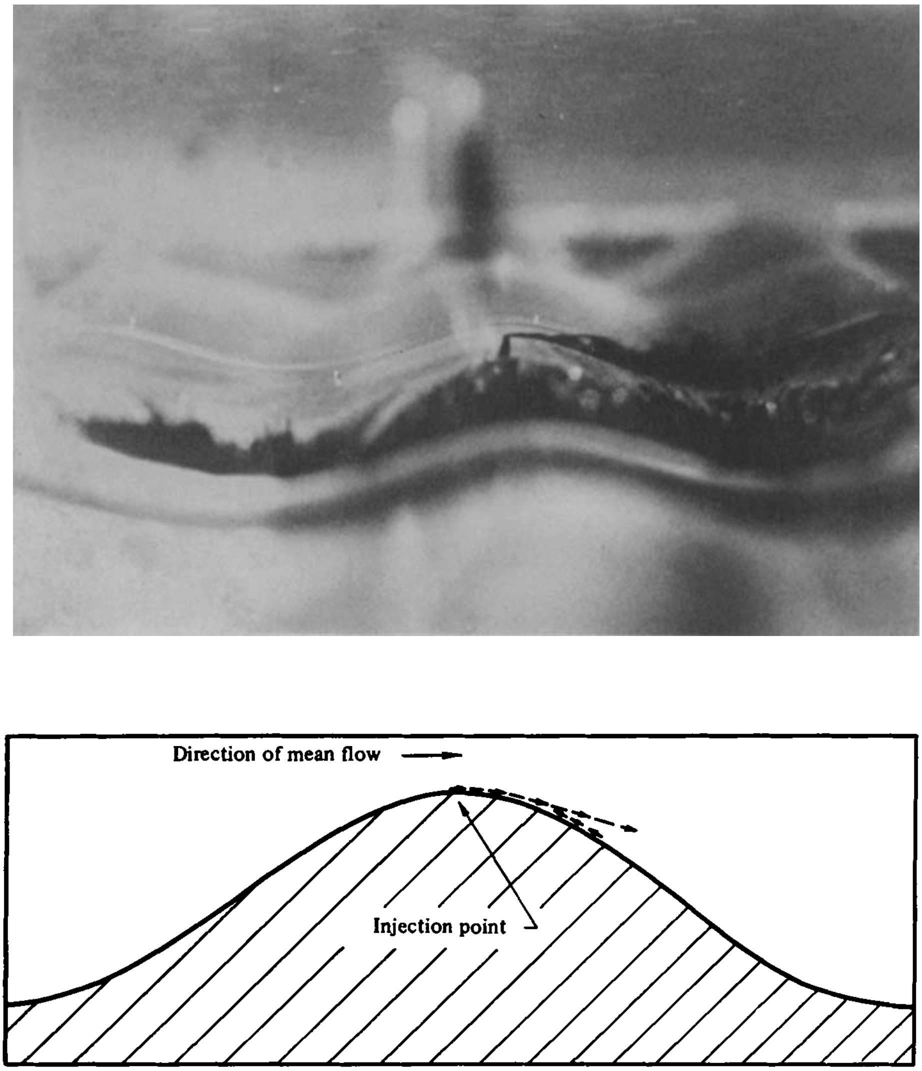

FIGURE 1 (*b*). For legend see plate 4.

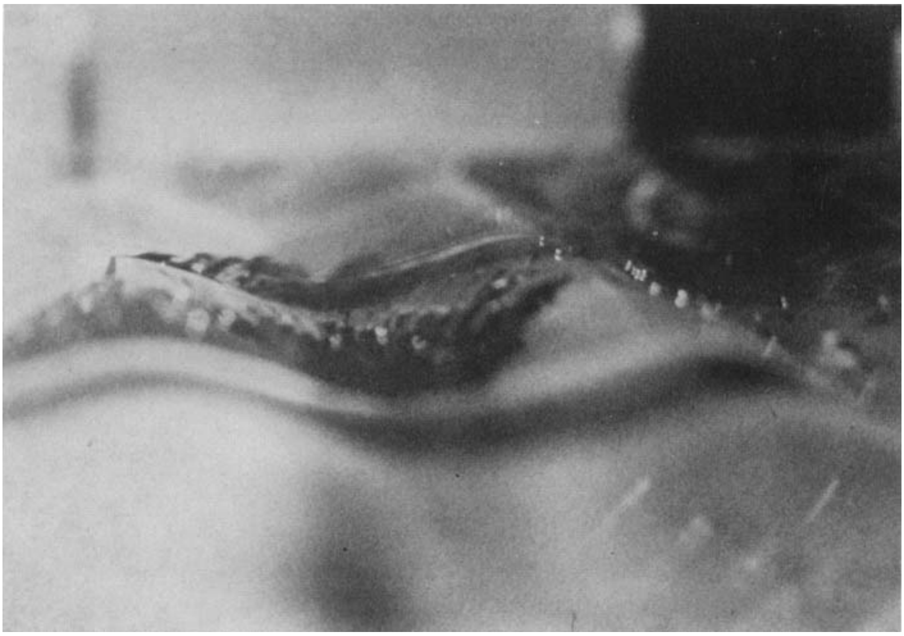

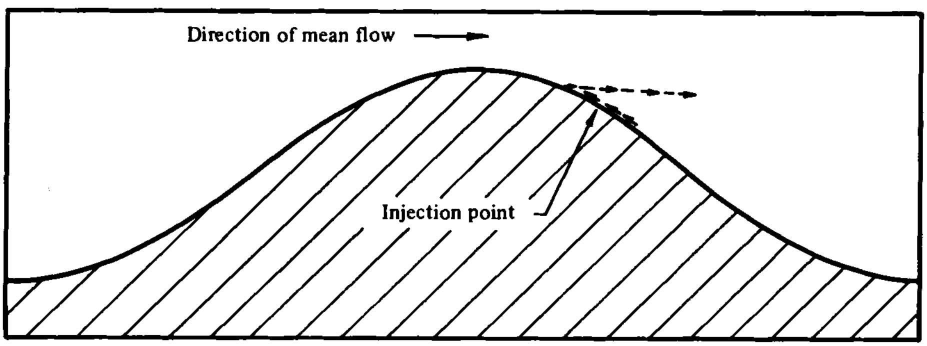

FIGURE 1 (*c*). For legend see plate 4.

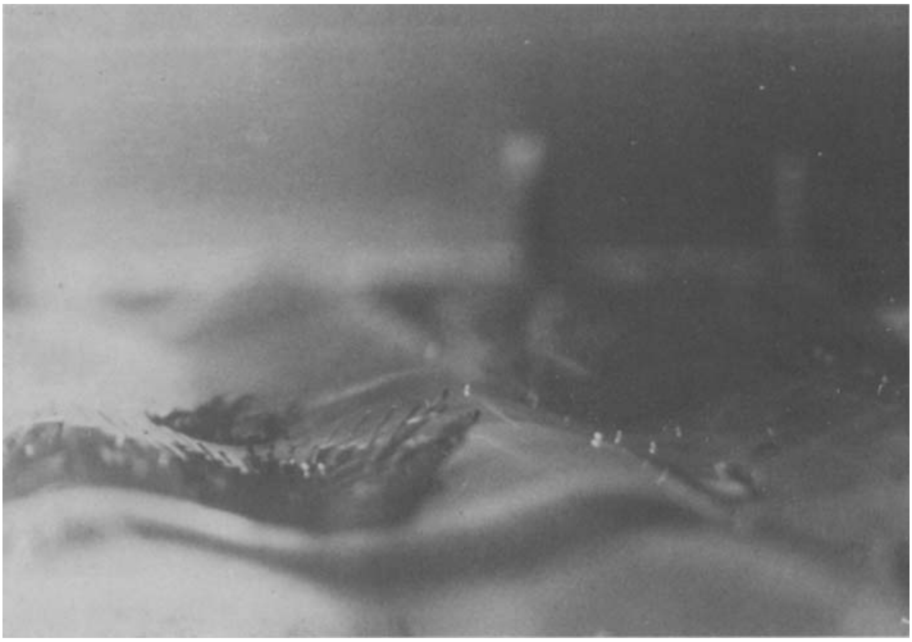

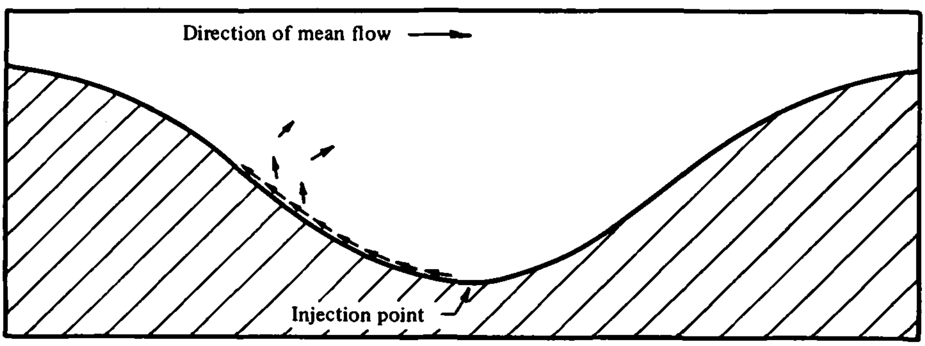

FIGURE 1. Dye streamers resulting from injection (*a*) in the forward region, (*b*) near the separation point, (*c*) downstream of the separation point and (*d*) near the wave trough.